

# Toward a Better Understanding of Blast Furnace Raceway Blockages

Stefan Puttinger\* and Hugo Stocker

Operational data of two small size blast furnaces (BFs) with respect to the occurrence of raceway blockages are analyzed. These blockages mainly occur due to erratic movements in the burden. In a previous project, the authors have investigated the various types of raceway blockages and tested different approaches to implement a reliable way to detect such blockages at a very early stage. Early detection of severe blockage events is important to avoid tuyere damages and trigger operational reactions like, e.g., the shutdown of pulverized coal injection (PCI) branches. The most promising algorithm of the previous project has been implemented in the process control system of the BFs and enhanced with the additional calculation of a strength factor serving as an indicator for the severity of a blockage event. The system is now collecting data on raceway blockages since the beginning of 2019. As there is now a good data basis available, herein, the latest findings on blockage event statistics and the correlation with other operational data of the BF are presented.

## 1. Introduction and Motivation

Around 69% of the worldwide steel production is still based on pig iron production through the blast furnace (BF) route.<sup>[1]</sup> Although the overall process and the chemical reactions inside a BF are well understood, it still remains a sort of black box when it comes to local flow conditions and the movement of solid particles, gas, and liquids inside. Thus, there are a lot of issues during BF operation which cannot be fully explained on the basis of the available measurement data. One of these issues is the irregular movements of the burden. Sometimes the descent of the burden comes to a stop or suddenly drops down even for a few meters. This behavior is

usually termed “hanging” and “slipping.”<sup>[1]</sup> Hanging and slipping of the burden can occur as local effects influencing only one or several neighboring tuyeres or can also appear on a large scale covering major parts or the entire BF. It can locally change the permeability of the burden and cause asymmetries in the BF, and they are also assumed as one of the reasons for the frequent occurrence of raceway blockages that can affect one or several tuyeres.

Although, the reasons for hanging and slipping are yet not fully understood, there are some possible explanations for this behavior. From the theory of granular media, it is known that particles form force chains.<sup>[2,3]</sup> This arching effects are of major interest for the discharging of granular material from hoppers as they can cause jamming and avalanching.<sup>[4–6]</sup> For mono-

disperse spherical material, the probability of jamming during hopper discharge is influenced by the ratio of particle diameter and the outflow diameter.<sup>[3]</sup> However, for technically relevant materials the formation of force chains is also influenced by the shape of the particles,<sup>[7–9]</sup> and the differences in particle sizes for nonmonodisperse materials.<sup>[10]</sup> In a lab-scale environment, these force chains can also be visualized experimentally.<sup>[11]</sup>


Comparably, counter-current reactors like BFs are also affected by arching and avalanching effects. All granular materials inside have an irregular shape and a wide distribution of particle sizes from the range of centimeters (coke and sinter) down to the micrometer range (dust and unburned coal particles from pulverized coal injection [PCI]). Especially, the cohesive zone is prone to form force chains and arching as the melting iron tends to glue particles together on one side and the consumption of coke and ore also produces additional voidage.

A second reason for irregular burden movements is scaffolds at the furnace walls. These can be formed when alkali- or zinc-rich components are vaporized in the lower hot areas and then condensate at the cooler walls. These scaffolds locally alter the gas and temperature distribution. Eventually, these structures will break off the walls when they become too large, especially when there are void regions formed below due to the consumption of coke.

Although there are hundreds of measurement signals nowadays, there is still very few information available what is really going on inside the BF. Most data are temperature and pressure signals or signals related to the mass flow rates of burden and coke charged at the top, liquid iron and slag tapped from the bottom and the hot blast flow rates. There are basically only two regions where information can be obtained from inside the BF—the

Dr. S. Puttinger  
Department of Particulate Flow Modelling  
Johannes Kepler University  
Altenbergerstrasse 69, 4040 Linz, Austria  
E-mail: stefan.puttinger@jku.at

H. Stocker  
Research and Development  
voestalpine Stahl Donawitz GmbH  
Kerpelystrasse 199, 8700 Leoben, Austria

 The ORCID identification number(s) for the author(s) of this article can be found under <https://doi.org/10.1002/srin.202000227>.

© 2020 The Authors. Published by WILEY-VCH Verlag GmbH & Co. KGaA, Weinheim. This is an open access article under the terms of the Creative Commons Attribution-NonCommercial License, which permits use, distribution and reproduction in any medium, provided the original work is properly cited and is not used for commercial purposes.

DOI: 10.1002/srin.202000227

burden fill level at the top of the BF and the visual information of the raceway areas through the tuyere inspection windows. Information about the burden height can be derived from point-wise measurements via mechanical stockrod probes or microwave sensors,<sup>[12]</sup> 3D radar systems,<sup>[13,14]</sup> or, more recently, also the 3D reconstruction of the burden from optical sensors.<sup>[15,16]</sup> If the burden measurement system has a sufficient time resolution also the downward movement of the burden can be tracked.

Concerning the raceway itself there is mainly pressure signals available which give the flow rate of hot blast on every tuyere. In addition, there is the visual information from the peepholes but inspection is mainly done manually by the operating personal on an arbitrary basis. However, due to the rapid development in camera technology, some furnaces have been extended with a permanent camera installation delivering continuously image data from the tuyeres. This visual information is invaluable to better understand the transient behavior of hot blast flow rates and the appearance of different types of raceway blockages.<sup>[17–19]</sup> To give two examples, **Figure 1a** shows a normal raceway behavior, and **Figure 1b** shows an entire blockage of the tuyere. Further examples of raceway blockages are given in the previous paper.<sup>[17]</sup>

In the previous publication, we conducted a feasibility test where we were processing 1500 h of BF data in a test environment to check if the system runs stable and delivers useful results.<sup>[18]</sup> At that time, we were only detecting blockage events regardless of it were only short- or long-lasting blockages. To gain more information, we enhanced our system in the meanwhile to also account for the strength of a blockage event. After implementation of the proposed signal processing method in the process control system, it is continuously recording data since May 2019. In this study, we now make use of the collected data over a time range of 10 months to analyze the relation of raceway blockages and sudden movements in the burden in more detail. Note that, all data in this article are given in a non-dimensional, normalized form. However, the qualitative information was conserved, and the figures are kept clear and easy to interpret.

## 2. The Blockage Detection System

We have previously compared various strategies to reliably detect raceway blockages.<sup>[17–19]</sup> A blockage in front of the tuyere will

cause a reduction on hot blast flow rate and will be recognizable in the pressure signal of that tuyere. However, the most common implementation of simply thresholding the pressure signals lacks of accuracy due to deviations between the tuyeres and sensor drifts due to ageing effects, sensor damage, or other electrical issues. To improve the blockage detection rate, we have tested more robust signal processing strategies.<sup>[18]</sup> Although a human operator can easily distinguish between an ordinary raceway situation and an abnormal behavior, it is a difficult task to find blockage events in an image series via classical means of image processing.<sup>[19]</sup> The brightness and contrast of the images varies strongly with PCI rates and temperature and, therefore, automatic processing of the camera data is not straight forward. Machine learning methods have not been tested yet, but will be investigated in future activities.

The data used in this study are obtained from BFs BF1 and BF4 at voestalpine Stahl Donawitz GmbH. Both furnaces do not have a permanent camera installation. Only temporary cameras on single tuyeres have been used to obtain validation material for the tested algorithms. As an outcome of the previous study an algorithm based on short- and long-term filtering of the hot blast signals has been implemented in the process control system. This algorithm was labeled A2 in the previous paper.<sup>[18]</sup> We will give a short summary of the signal processing procedure here, and **Figure 2** shows the procedure for one of our test case signals.

The algorithm is based on the comparison of a short- and a long-term filtering of the tuyere pressure signals. It calculates a weighted average with two different weight factors  $w_S$  and  $w_L$ ,

$$\bar{x}_{S,k} = x_k \cdot w_S + (1 - w_S) \cdot \bar{x}_{S,k-1} \quad (1)$$

$$\bar{x}_{L,k} = x_k \cdot w_L + (1 - w_L) \cdot \bar{x}_{L,k-1} \quad (2)$$

for short- and long-term averaging, respectively. The signal  $x_k$  is the most recent sample of the tuyere pressure signal (which corresponds to the hot blast flow rate). The weight factors are set to  $w_S = 0.2$  and  $w_L = 0.02$ . A small weight factor means, that the influence of the most recent sample on the average  $\bar{x}_{L,k}$  is low, thus we have a long-term filtering, a larger weight factor increases the influence of the most recent value and we obtain a short-term filtering  $\bar{x}_{S,k}$ . This weighted averaging can also be interpreted as

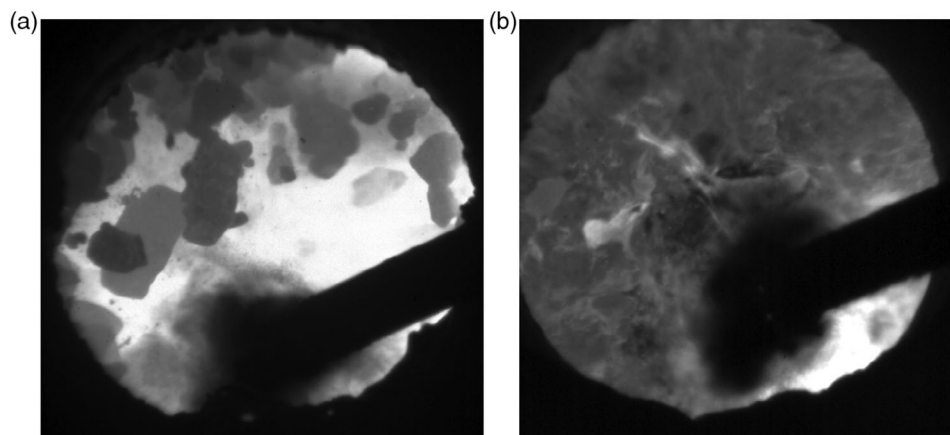


**Figure 1.** a) Example of normal raceway operation and b) complete blockage of the raceway.

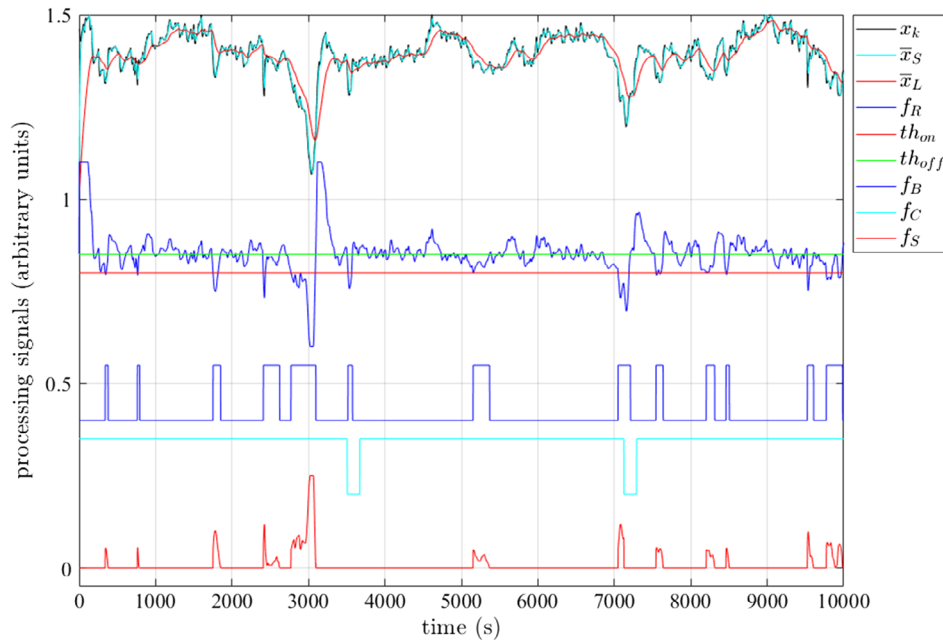


**Figure 2.** Example for the calculation of the blockage and strength signal:  $x_k$  is the tuyere hot blast flow rate signal,  $\bar{x}_S$  and  $\bar{x}_L$  are the short- and long-term filtered signals,  $f_R$  is the result signal based on the ratio  $\bar{x}_S/\bar{x}_L$ . The blockage signal  $f_B$  is obtained by thresholding  $f_R$  with  $th_{on}$  and  $th_{off}$ . Multiplying of  $f_R$  and  $f_B$  and  $f_C$  which indicates the switching of the hot blast stoves, finally delivers strength the signal  $f_S$ . The figure legend represents the line types in the correct order from top to bottom.

low-pass filtering of the signal with two different cut-off frequencies. The ratio of short- and long-term filtering results

$$f_R = \frac{\bar{x}_S}{\bar{x}_L} \quad (3)$$

is a good indicator for time periods where  $\bar{x}_S$  strongly deviates from  $\bar{x}_L$ . This is the case when blockages in front of the tuyere rapidly reduce the hot wind flow rate. Applying appropriate threshold levels on  $f_R$  finally delivers the digital blockage signal  $f_B$ . As  $f_R$  is normalized, the threshold levels are now independent of the strongly deviating mean signal levels of  $x_k$  on the individual tuyeres (which might be caused by signal drift, sensor ageing effects, etc.).

The algorithms have been validated against several test data sets, which consist of the real tuyere pressure signals from the BF plus additional image data from temporarily installed tuyere cameras. Out of these image data, a reference signal vector has been extracted, marking every blockage event a human operator would identify as such. The filter weight factors  $w_S$  and  $w_L$  and the threshold levels ( $th_{on} = 0.935$  to activate the blockage signal and  $th_{off} = 0.98$  to deactivate it) have then been optimized manually to reach the highest match and lowest false-detection rates on the test data.

The system has then been further extended to provide not only a yes/no signal if a blockage is present or not, but also additional information about the strength of an event. The strength signal  $f_S$  (red line at the bottom of Figure 2) is generated by taking the absolute value of the result signal  $f_R$  and doing a sample-based multiplication with the digital blockage signal  $f_B$  and the digital

signal  $f_C$  which indicates the switching events of the hot blast stoves

$$f_S = |f_R| \cdot f_B \cdot f_C \quad (4)$$

In the online system, each detected event is stored in a database with a unique event id. Every database entry consists of the following information: 1) tuyere number; 2) start time of event; 3) end time of event; 4) duration in seconds; and 5) strength of event.

The latter value is calculated by integrating the strength signal  $f_S$  for each event between the start and end time. Doing so will produce a high value for all long events—also if the reduction of hot blast flow rate is not that high—and also for shorter events where the reduction of the wind flow rate is very strong. The resulting scalar value is therefore a good indicator for the severity of a raceway blockage event.

In the previous publication, we conducted a feasibility test on  $\approx 1500$  h of operational data of BF1. In this quasionline test, the data were read from a database and processed in our test environment.<sup>[18]</sup> As it was running stable and delivering consistent results, the proposed method of signal processing was implemented in the online process control system and finally enhanced with the calculation of the strength factor. After an initial testing and optimization phase, the system is now continuously recording data since May 2019. As everything is based on the hot blast flow rate signals, the blockage signals and event statistics can also be recalculated offline by exporting the flow rate signals from the process control system. This is done on a regular basis to cross-check the results and test different parameter sets.

### 3. Results and Discussion

#### 3.1. Long-Term Statistics on Raceway Blockages

The blockage event data presented in this section were collected in the period from May 2019 until March 2020 on BF1 and BF4 at voestalpine Stahl Donawitz GmbH which have 20 tuyeres each. In total, the system has recorded 312.725 events on BF1 and 221.876 on BF4, respectively. These numbers appear quite large, and indeed we have stored every detected event (also very short ones) in the database to obtain a complete picture. Although it is known that there are frequent blockages of the raceway, very short blockages are usually not recognized by the operating staff. Thus, the total number of events is surprisingly high, even if we account for a false-detection rate of  $\approx 10\%$ . Table 1 shows the comparison between the average number of blockages per hour and day for the whole furnace and per tuyere. The third column in Table 1 shows the corresponding numbers from the formerly published data of the test system.<sup>[18]</sup> It demonstrates that the currently implemented online system is fully consistent in its results with the data from the proof-of-concept tests (these tests were only conducted on data from BF1). The average number of

**Table 1.** Average number of detected blockage events. The last column refers to the previously published data and demonstrates that the currently implemented online system is consistent with the proof of concept on a test system (data available only for BF1).<sup>[18]</sup>

BF	BF1	BF4	BF1
Data period	May 2019– March 2020	May 2019– March 2020	January 2018– March 2018
Blockage events per hour	41.5	29.4	43.5
Blockage events per hour per tuyere	2.07	1.47	2.17
Blockage events per day	995	706	1044
Blockage events per day per tuyere	49.7	35.3	52.2

detected blockages is essentially the same in the final implementation.

Figure 3 shows the number of recorded events per tuyere. Both furnaces have one taphole which is located between tuyere 1 and 20 to give an orientation of the diagram. The number of blockage events is not evenly distributed around the circumference of the BFs. There are tuyeres which show indeed the double number of detected blockages (e.g., tuyeres 2 and 12 on BF1) than on other tuyeres (c.f. tuyeres 4 and 17 on BF1). This indicates that there are inherent asymmetries in the furnaces. There are no obvious reasons for such asymmetries, however, there are a few assumptions how this behavior can be explained. One reason could be that local differences in the permeability of a particle bed tend to reinforce themselves. A higher porosity leads to a locally decreased pressure drop and thus a higher percentage of gas flow is passing through the higher porosity zone and enforces segregation and channeling effects. This behavior is well known from fluidized bed reactors.<sup>[20,21]</sup> However, local deviations in the permeability cannot explain the persistent differences between the tuyeres on the long term. In a BF, the active coke zone has a higher porosity than the cohesive zone, thus, the air flow rising from the raceways is typically deflected toward the center of the BF. To alter this average flow behavior, it needs longstanding or repeatedly occurring local deviations in the bed structure. For example, scaffolds above a tuyere lead to an increased deflection of the gas flow toward the center of the BF.<sup>[22,23]</sup> Deflections toward the circumference could be caused by bird's nest structures due to the accumulation of unburned coal particles in the coke bed or an asymmetric geometry of the dead man (which is usually assumed to be a cone-like structure).<sup>[24,25]</sup>

Apparently, there are large differences between the two BFs. The recorded data show 41% more blockage events on BF1 than on BF4. There are two possible reasons for these differences. The two furnaces are not completely identical. BF4 has a larger hearth volume. As a consequence, the pool of liquid iron exerts a

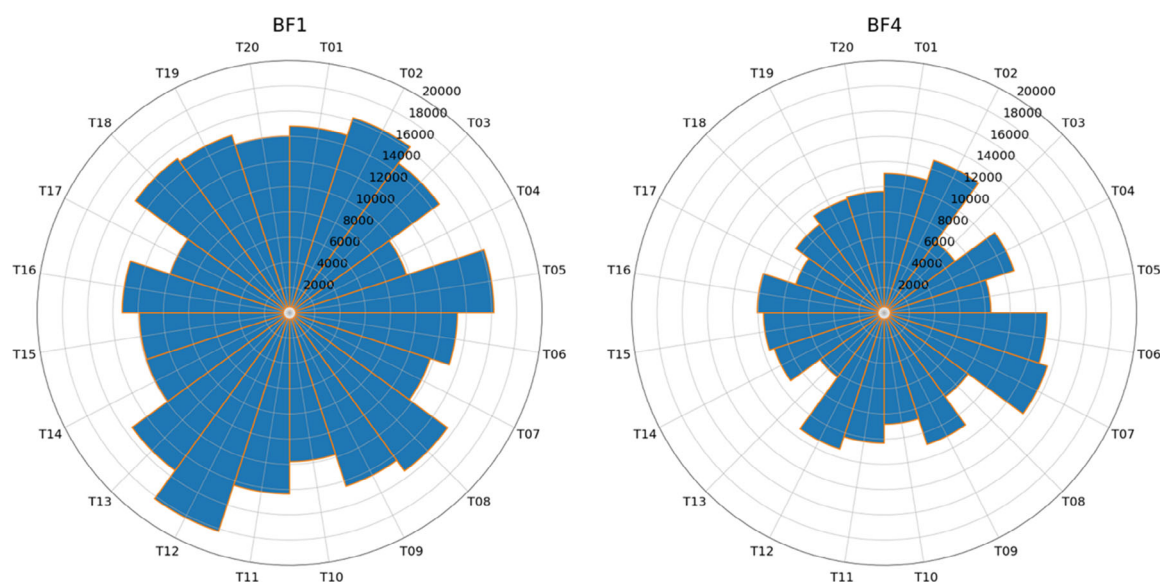


**Figure 3.** Total number of blockage events per tuyere for BF1 (left) and BF4 (right) in the period May 2019 to March 2020.



larger buoyancy force on the dead man as coke has a much lower density than liquid iron. Thus, BF4 has a stronger tendency for a floating dead man than BF1. If we stick to the assumption that the dead man is a cone-like structure one conclusion is, that if this structure is moved upward the hot blast gas flow distribution at the tuyere level will be altered. In which manner is hard to predict as it is not clear in what area the porosity will be higher. The coke bed in the dead man is usually assumed to have a porosity of 0.35.<sup>[26]</sup> If there is no deposition of fines in the dead man area (the formerly mentioned bird's nest effect), the coke bed in the dead man will most likely have a higher porosity than the descending burden (especially the cohesive zone). This would lead to a more centrally oriented gas flow. If the opposite is the case and the dead man accumulates unburned coal particles and other fines resulting in a low porosity, the flow will be deflected toward a ring-like area closer to the wall. The differences between a wall working and a central working furnace are illustrated by Geerdes et al.<sup>[1]</sup>

A second difference between BF1 and BF4 is the age of the lining. Both furnaces undergo an alternating partial relining every 4 years, which means that the refractories of BF4 are 2 years longer in operation. Presumably, the erosion of the lining on BF4 is larger than on BF1 and BF4 has a larger inner diameter and a more irregular shape of the outer walls. The used burden material is rich of alkali (the average load for 2017 was  $7.8 \text{ kg thm}^{-1}$ ) which increases erosion and the tendency to form scaffolds. Hence, this is another factor which can influence the flow distribution between the central area and the wall region.

Figure 4 might give additional information to understand the differences between BF1 and BF4. It shows the number distribution of recorded blockage strengths. The vast majority of recorded blockage events are weak events. The total number of strong events is actually very low. Figure 4 also shows that the difference in the total number of events between BF1 and BF4 is mainly caused by a different frequency of occurrence of weak events. In addition to the first bar of the lowest strength values, the remaining distribution is almost the same for both BF's. This is another indicator that there is a different flow distribution in the two furnaces. From a fluid mechanics

perspective, it is plausible that a persistent difference in the average flow situation (which could be caused by, e.g., a floating dead man in one furnace and a sitting dead man in the other) can influence the number of short blockages on the long run. As discussed earlier, a higher inertia around the raceway will alter the local force balances and push smaller agglomerates of material away and keep the tuyere free of blockages. However, these minor differences on the global flow distribution are not likely to influence large-scale movements of the burden. Consequently, the number of strong blockages is almost identical for both furnaces.

### 3.2. Coupling of Neighboring Tuyeres

The blockage detection system treats every tuyere individually. However, it can be assumed that a blockage on one raceway could be caused not only by a local movement in the bed, but also by large-scale movements of the burden. Thus, most likely neighboring raceways will show a similar behavior and high correlation of blockage events.

Figure 5 shows the correlation matrix of the tuyeres for the daily number of events on BF1 and BF4. Along the main diagonal, we see that each tuyere has a coupling with its ultimate neighbors. This means that a certain number of blockages does affect more than one raceway area. Especially, the area around the taphole (which is located between tuyere 20 and 1) shows higher correlations on both furnaces. On BF1, the tuyeres 18, 19, 20, 1, 2, and 3 have a strong coupling, whereas this area is less pronounced on BF4 (tuyeres 20, 1, and 2) but still stronger correlated than the rest of the tuyeres. BF1 also shows a larger block of correlated blockage events between tuyeres 3 and 9. Off the main diagonal, the correlation coefficients between the tuyeres are lower on BF4 than on BF1. For BF1, we can identify some areas off the diagonal with a correlating frequency of occurrence of blockages. Figure 5a even shows an X-like structure in the correlation matrix. Blockages on tuyeres 4–6 are related to blockage events on tuyeres 13–15, which are located at the opposite side of the furnace. Likewise, there is a high correlation of tuyeres 8 and 9 with tuyeres 12 and 13. This behavior is caused by the increased

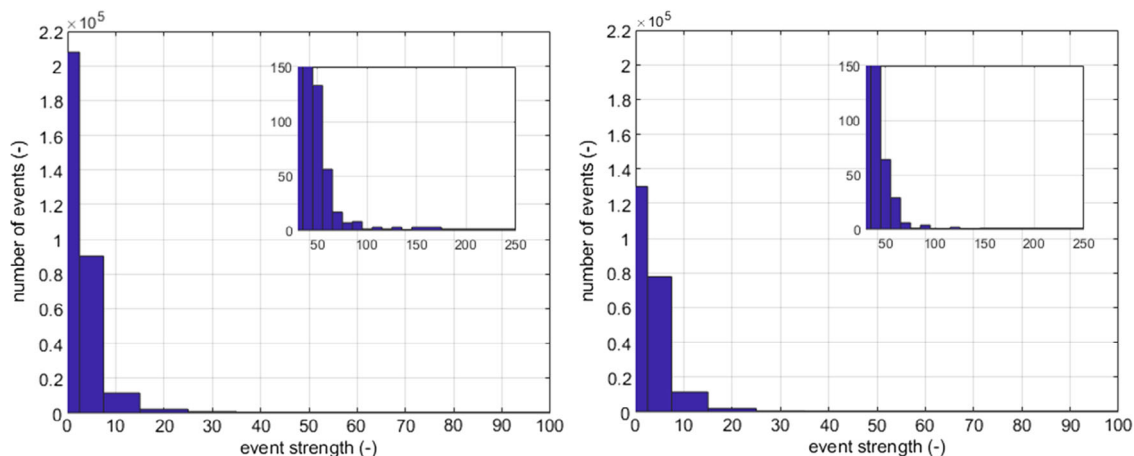


**Figure 4.** Distribution of blockage strength for BF1 (left) and BF4 (right) in the period May 2019 to March 2020. The insets show the zoomed range of strong events.

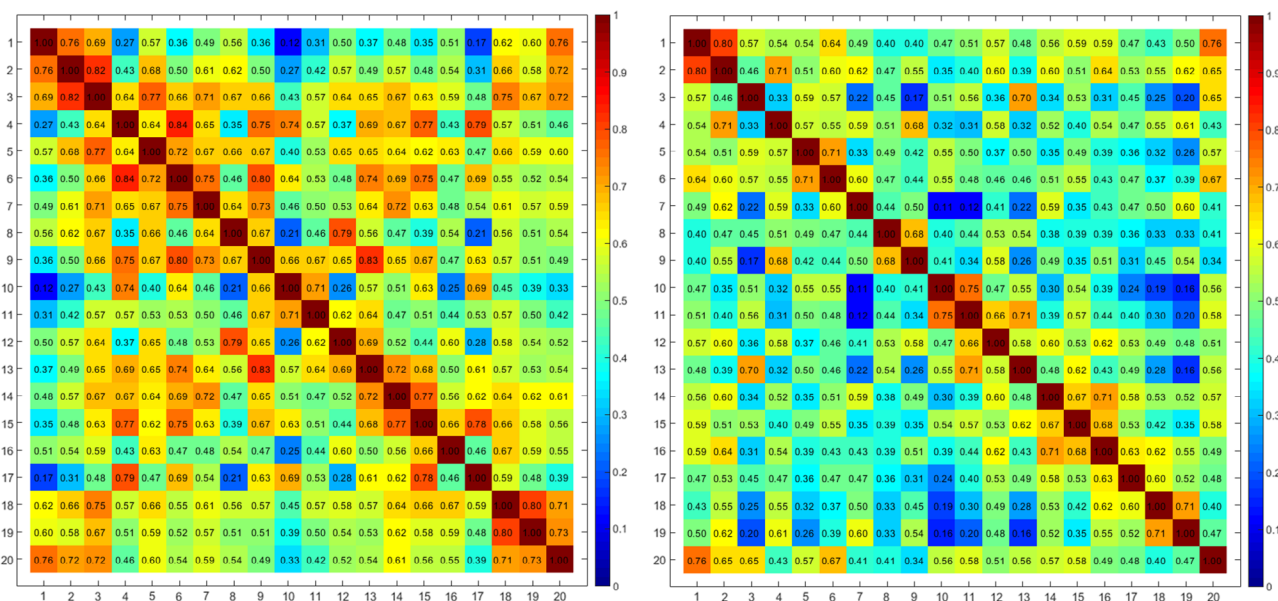


**Figure 5.** Correlation matrix for the daily averages of the number of events on BF1 (left) and BF4 (right).

number of blockages in the neighborhood of tuyeres 7 and 14 which was caused by the temporary plugging of these tuyeres that is discussed in more detail in Section 3.3.

It is also interesting to note that tuyere 4 has a stronger correlation with other tuyeres around the furnace which are not in the proximity of the tuyere (e.g., tuyeres 9, 15, and 17). According to Figure 3, tuyeres 4 and 17 are among the tuyeres that show the lowest numbers of blockage events. Our interpretation of a low number of blockages but high correlation coefficient is that these tuyeres are mainly affected by larger movements in the burden (which are more likely to be strong events). This presumption is substantiated by the fact that the number of weak events (strength value 1, c.f. Figure 4) is around 7000 for these two tuyeres, whereas it is above 10 000 for other tuyeres. However, one has to be careful in interpreting such correlation coefficients as there is not necessarily a physical reason for correlations in the data. These can also simply be triggered by coincidence and need to be further investigated. The main conclusion from Figure 5 is that each tuyere has a coupling with its neighbors and thus the number of blockages spanning two or three tuyeres is high.

### 3.3. Correlation of Raceway Blockages with Large-Scale Burden Movements

To understand the relation of large-scale burden movements and raceway blockages, it is helpful to compare a period with smooth BF operation and a period with erratic behavior. Figure 6 and 7 shows an example for both cases. Figure 6 shows a period of smooth operation from July 2019 and Figure 7 an irregular phase from August 2019 where tuyeres 7 and 14 were closed. Both figures show a time plot of the tuyere pressure levels along with the furnace pressure (black line) and the two pointwise burden radar signals (red and blue lines). The furnace pressure signal indicates two phases of shutdown for revisions in Figure 7.

The average number of events per day is almost equal (1188 for the time period shown in Figure 6, 1127 for Figure 7), however, there is a significant difference on the number of strong events. During smooth operation, the vast majority of events was weak, and there was only one event recorded with a strength level  $>20$  (c.f. the strength distribution shown in Figure 4). In contrast, there were 192 strong blockage events detected during the time period shown in Figure 7. It is evident that the absence of gas flow and raceways on the two closed tuyeres has a negative impact on the burden movement in the area between them. There is a significant increase in strong blockage events, and the blockages tend to occur on multiple tuyeres at the same time. We can assume that the plugging of the two tuyeres intensifies erratic burden movements, and these movements occur on a larger scale, affecting the whole area between the closed tuyeres.

It is highly interesting that, despite the fact that there is a vertical distance of  $\approx 25$  m between the tuyere level and the burden level, the movements on top of the burden still correlate well with the blockages detected at the tuyere level which can be seen from the stockrod data. During normal operation, the burden radar shows fluctuations around an average fill level with some occasional larger descents of the burden (Figure 6). During the period shown in Figure 7, the radar signals show larger deviations and a higher occurrence of strong movements in the burden. This underlines that the plugging of the two tuyeres has a negative impact on the movement of the complete burden and enforces hanging and slipping.

### 3.4. Raceway Blockages as an Indicator for Tuyere Damages

Damages of the tuyeres are a significant cost factor and also imply some security risks due to the water leakage into the BF. Thus, the early detection of process states that can potentially

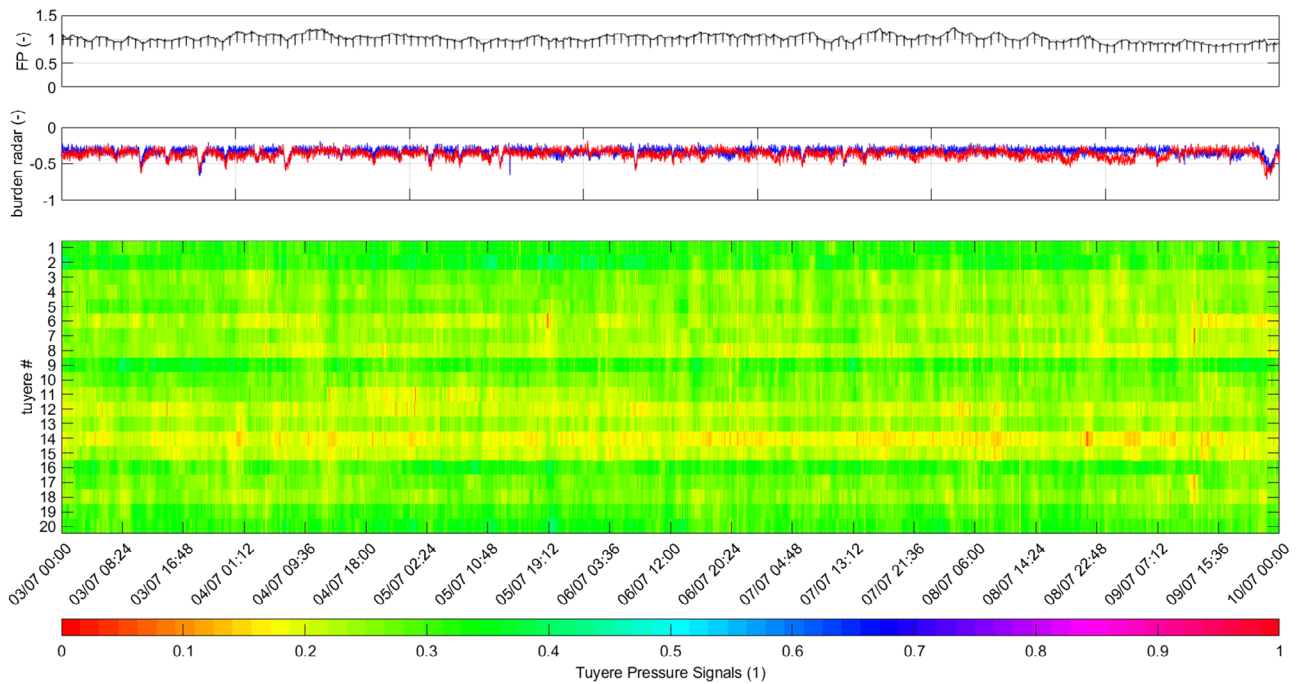


**Figure 6.** Period of smooth BF operation. The color plot provides the pressure levels on all 20 tuyeres of BF1 during the period July 3, 2019 to July 10, 2019. The red color indicates highly reduced or increased blast flow rates (due to blockages or channeling). In addition, the top line (black) is the furnace pressure and the red and blue curves are the two burden radar signals. All signals are normalized.

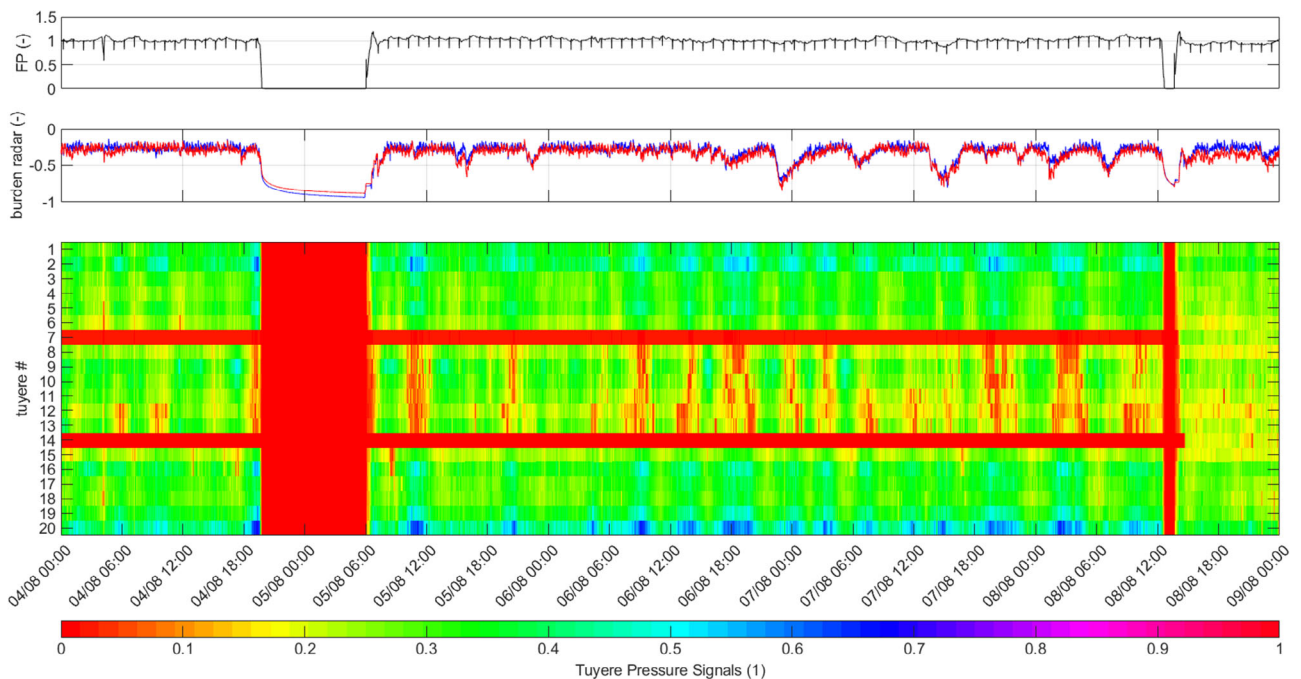


**Figure 7.** Erratic BF operation during a period where tuyeres 7 and 14 have been plugged. The color plot provides the pressure levels on all 20 tuyeres of BF1 during the period August 4, 2019 to August 9, 2019. The red color indicates highly reduced or increased blast flow rates (due to blockages or channeling). In addition, the top line (black) is the furnace pressure, and the red and blue curves are the two burden radar signals. All signals are normalized.

lead to tuyere damages would be highly beneficial for BF operation. The operators could take countermeasures to prevent the

damage, or, if this is not possible, schedule an early replacement of the tuyere in the sense of predictive maintenance.

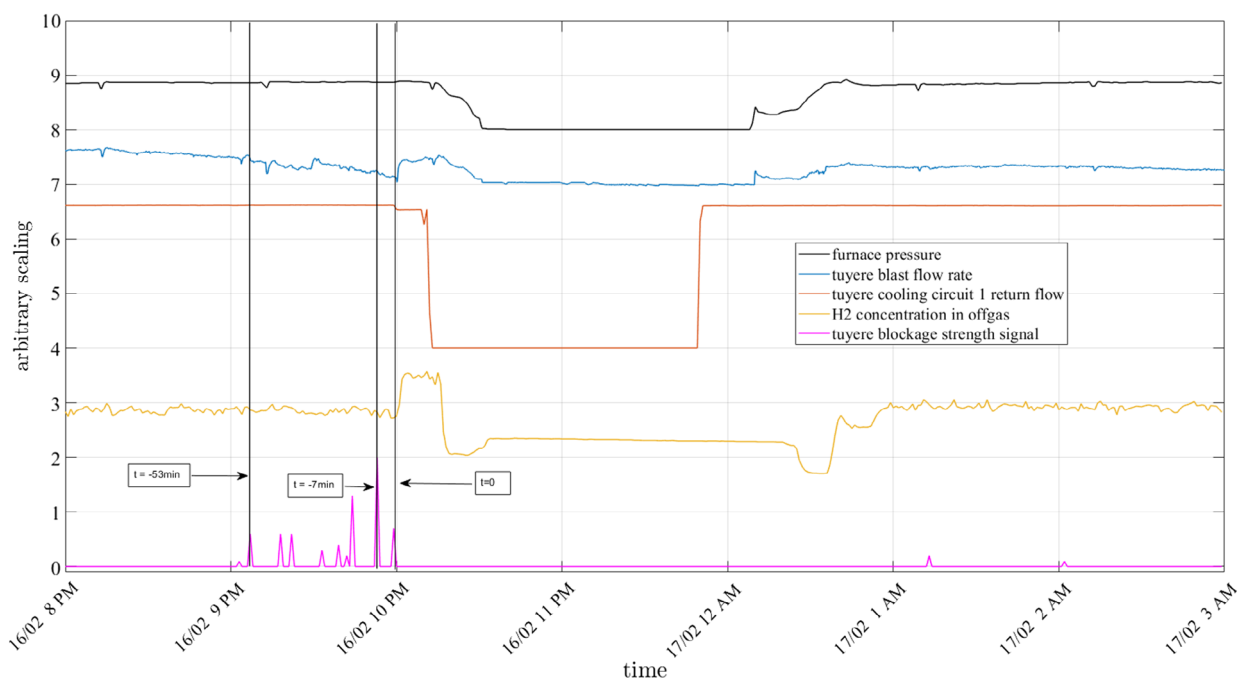


**Figure 8.** Example of the blockage strength signal right before a tuyere damage with water leakage into the BF. A first reduction of the return flow rate is visible at 10 pm. This is also the point where the H<sub>2</sub> concentration in the top gas starts to increase, which indicates a water leakage into the furnace. A major blockage event was recorded 7 min before the leakage, and the first event of the series of blockages was detected 53 min ahead of the tuyere damage.

Figure 8 shows an example of a tuyere damage on February 16, 2020. The signals show the detected blockages (magenta) along with the furnace pressure (black), the tuyere hot blast flow rate (blue), the water flow rate of the tuyere cooling circuit (red), and the measured H<sub>2</sub> concentration in the top gas (yellow). At 10 pm, we see a slight reduction of water flow in the cooling circuit. This is the same time, where the H<sub>2</sub> concentration in the top gas starts to increase, thus, we can assume a water leakage from the tuyere into the BF. A major blockage event was recorded 7 min ahead of the leakage. This correlation was also observed for several other tuyere damages. Even more interesting is the fact, that the series of blockage events actually starts much earlier. In the shown example, the first stronger event was detected 53 min ahead of the water leakage. In other cases, we observed an increase in blockage events up to 90 min before the actual tuyere damage. Thus, the blockage detection system can be used to generate warning signals for the operators to have a closer look on a specific tuyere or start preparations for the next shutdown phase to replace the damaged equipment.

#### 4. Conclusions and Outlook

Currently, the phenomenon of frequent raceway blockages inside a BF is not fully understood. In this article, we discussed the results of an improved raceway blockage detection system based on the signal analysis of the hot blast flow rate data of the individual tuyeres. This system was validated against temporary tuyere camera installations in a previous study and finally

implemented in the process control system of two small-size furnaces at voestalpine Stahl Donawitz GmbH in 2019. The data presented in this article cover a time span of 10 months from May 2019 to March 2020. These data now allow to do long-term statistics of blockage events and to test the relation of these blockages with other process parameters. Our main conclusions from the collected data so far are: 1) the actual number of blockages is quite big; however, the majority of blockage events is rather short and not critical concerning potential damage of the tuyeres. 2) Despite the large vertical distance between the raceway zone and the burden top, there are periods with clear correlation between sudden movements of the burden at the top of the furnace and the strength of tuyere blockages. Thus, many tuyere blockages are not caused by only local effects in the raceway but can be triggered by large-scale motions in the burden due to hanging and slipping. 3) This fact can also be deduced from the correlation of neighboring tuyeres. Larger movements in the bed are likely to affect several raceway areas within a certain time span. 4) The accumulation of strong raceway blockages is a good indicator for potential tuyere damages. The collected data show that the number and strength of blockages was increasing right before the damages occurred. Future test will show, if the blockage signals can be used as an indicator for predictive maintenance measures.

Future activities should be focused on two major issues: i) further data analysis to test for correlations of the blockage events with other process parameters, ii) implementation of the system on a larger BF to see if there are significant differences in the frequency of occurrence of raceway blockages.



## Acknowledgements

The authors gratefully acknowledge the funding support of K1-MET GmbH, metallurgical competence center. The research programme of the K1-MET competence center is supported by COMET (Competence Center for Excellent Technologies), the Austrian programme for competence centers. COMET is funded by the Federal Ministry for Climate Action, Environment, Energy, Mobility, Innovation and Technology, the Federal Ministry for Digital and Economic Affairs, the Federal States of Upper Austria, Tyrol and Styria as well as the Styrian Business Promotion Agency (SFG). Beside the public funding from COMET, this research project is partially financed by the scientific partner Johannes Kepler University Linz and the industrial partner voestalpine Stahl Donawitz GmbH.

## Conflict of Interest

The authors declare no conflict of interest.

## Keywords

blast furnaces, blockage detection, raceway monitoring

Received: April 27, 2020

Revised: May 28, 2020

Published online: June 23, 2020

- 
- [1] M. Geerdes, R. Chaigneau, I. Kurunov, O. Lingiardi, J. Ricketts, *Modern Blast Furnace Ironmaking*, IOS Press/Authors, Amsterdam **2015**.
- [2] J. P. Wittmer, P. Claudin, M. E. Cates, J.-P. Bouchaud, *Nature* **1996**, 382, 336.
- [3] K. To, P.-Y. Lai, H. K. Pak, *Phys. Rev. Lett.* **2001**, 86, 71.
- [4] P. Mort, J. N. Michaels, R. P. Behringer, C. S. Campbell, L. Kondic, M. Kheiripour Langroudi, M. Shattuck, J. Tang, G. I. Tardos, C. Wassgrenk, *Powder Technol.* **2015**, 284, 571.
- [5] J. Xue, S. Schiano, W. Zhong, L. Chen, C.-Y. Wu, *Powder Technol.* **2019**, 358, 55.
- [6] Y. Li, N. Gui, X. Yang, J. Tu, S. Jiang, *Powder Technol.* **2016**, 297, 144.
- [7] N. Govender, D. N. Wilke, C.-Y. Wu, J. Khinast, P. Pizette, W. Xu, *Chem. Eng. Sci.* **2018**, 188, 34.
- [8] N. Gui, X. Yang, J. Tu, S. Jiang, *Powder Technol.* **2017**, 314, 140.
- [9] J. Tian, E. Liu, *Powder Technol.* **2019**, 354, 906.
- [10] T. F. Zhang, J. Q. Gan, A. B. Yu, D. Pinson, Z. Y. Zhou, *Powder Technol.* **2020**, 361, 435.
- [11] Y. Fang, L. Guo, M. Hou, *Powder Technol.* **2020**, 363, 621.
- [12] H. Saxen, M. Nikus, J. Hinnelä, *Steel Res.* **1998**, 69, 406.
- [13] D. Zankl, S. Schuster, R. Feger, A. Stelzer, S. Scheiblhofer, C. M. Schmid, G. Ossberger, L. Stegellner, G. Lengauer, C. Feilmayr, B. Lackner, T. Bürgler, *IEEE Sens. J.* **2015**, 15, 5893.
- [14] D. Zankl, S. Schuster, R. Feger, A. Stelzer, *IEEE Microw. Mag.* **2017**, 18, 52.
- [15] T. Xu, Z. Jiang, W. Gui, *IFAC-Pap.* **2018**, 51, 257.
- [16] T. Xu, Z. Chen, Z. Jiang, J. Huang, W. Gui, *Sensors* **2020**, 20, 869.
- [17] S. Puttinger, H. Stocker, *ISIJ Int.* **2018**, 59, 466.
- [18] S. Puttinger, H. Stocker, *ISIJ Int.* **2018**, 59, 474.
- [19] S. Puttinger, H. Stocker, *ISIJ Int.* **2018**, 59, 481.
- [20] S. Puttinger, S. Schneiderbauer, L. Von Berg, S. Pirker, *Procedia Eng.* **2015**, 102, 1752.
- [21] S. Schneiderbauer, S. Puttinger, S. Pirker, *Procedia Eng.* **2015**, 102, 1539.
- [22] T. Umekage, M. Kadowaki, S. Yuu, *ISIJ Int.* **2007**, 47, 659.
- [23] S. Yuu, T. Umekage, S. Matsuzaki, M. Kadowaki, K. Kunitomo, *ISIJ Int.* **2010**, 50, 962.
- [24] Y. Shen, T. Shiozawa, P. Austin, A. Yu, *Miner. Eng.* **2014**, 63, 91.
- [25] Y. Shen, A. Yu, P. Austin, P. Zulli, *Miner. Eng.* **2012**, 33, 54.
- [26] W. B. U. Tanzil, W. V. Pinczewski, *Chem. Eng. Sci.* **1987**, 42, 2557.